

Propagation of an aberrated wave with nonuniform amplitude distribution and its influence upon the interferometric measurement accuracy

R. JÓZWICKI

Institute of Design of Precise and Optical Instruments, Warsaw University of Technology, ul. Chodkiewicza 8, 02-525 Warszawa, Poland.

In interferometers with a nonzero difference of optical paths the propagating wave in the two paths changes differently. The difference of wavefront shapes gives the interferometric error induced by the aberrations. The formulae in a differential form describing the beam propagation with the planar and spherical wavefronts are derived. The results obtained are compared with the ones in the case of Airy beam propagation. The unfolding of the interferometric optical system with the reflecting surface is proposed. The influence of the illumination nonuniformity and primary aberrations is analysed. The cases of the Gaussian absorption are studied. The equation describing errors introduced by the aberrations of the propagating wave is found. The correction of the spherical aberration is formulated. The relation with the angular aberration is given.

1. Introduction

The influence of aberrations of an interferometric optical system on measurement results is known [1]–[3], [4] Sect. 6, and [5]. Interfering rays in the aberrated system change their direction with comparison to the theoretical one. Relevant changes of the optical paths of the rays occur and influence the measurement results. If the aberrations of the interferometric system are known, they can be taken into consideration. However, the analysis becomes complicated. Besides the changes of the optical paths of the rays, these rays displace in the interference field. The shear effect is different for different points of the field, and it can be significant for system with large difference of the optical paths. In this case, the fringe positions will depend on the position of a measured element in the test area. Usually, for this reason, the correction of aberrations of the interferometer system is good enough so that their influence can be neglected. The estimate of the influence of aberrations was made by an approximate method admitting an assumed maximum value of the changes of the optical path of the rays. The examination of an interferometer for eventual mounting faults is possible [4], Sect. 2.2.

Recently, the method of analysis of the influence of different phase defects of the whole interferometric optical system on the measurement error has been proposed [6]. The analysis is based on the optical path changes between a light source and a detector plane. The relation between the optical path changes and the wave aberration allowed us to find the expressions describing the changes of the wave coefficients introduced by the phase defects of the interferometer.

In the cases of precise measurements (accuracy $\lambda/50$ or better), especially for large differences of the optical paths of the interfering waves, the approaches mentioned above may be insufficient. The phase changes of the propagating wave depend not only on its wavefront shape but also on its amplitude distribution. The classical example is the propagation of the Gaussian beam in free space [7]. The amplitude distribution of the interferometric field does not have to be uniform, as, for example, in the case of a truncated laser beam illuminating an interferometer. To determine the influence of aberrations and nonuniform amplitude distribution of the interfering waves on the measurement results, we propose a new analytical and more natural approach. In the interferometric system the interfering waves are generated from the same original beam. The interfering waves meet in the interferometric field after passing different paths in the interferometer. On the propagation an aberrated wavefront changes. Because the distances of the wave propagation in the two paths are different, then the changes of the same wave in the two paths are different, too. So, the difference of the wavefront shapes of the interfering beams in the interferometric field is required to determine the measurement error introduced by the aberrations of the optical system. The formulae in a differential form describing the wavefront propagation will be derived. The estimation of the influence of the aberrations and nonuniform amplitude distribution will be given. The approach proposed allows us to determine the character of changes of the measurement results.

2. Statement of the problem

In interferometric system we have to deal with both the plane and spherical wavefront propagation. In the first case, the interferometer is used to test planar elements (Fig. 1a), and in the second case – the spherical ones (Fig. 1b). Let S and T be a standard and tested element, respectively. The interference occurs between waves reflected from surfaces d (wave 1) and b (wave 2) of the two elements. More exactly, we observe the interference of two waves generated from the same original wave 0, or, in other words, the interference of the same wavefront in two different

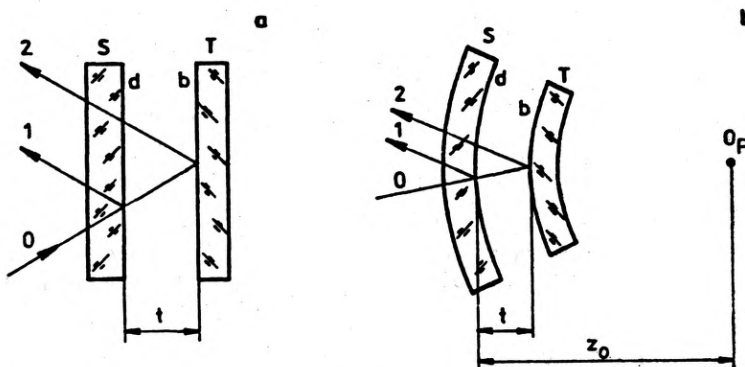


Fig. 1. Basic arrangement of the standard S and the tested element T in Fizeau interferometer for plane (a) and spherical (b) surfaces

moments. The original wave from an aberrated optical system not shown in Fig. 1 is divided by semitransparent surface d . To emphasize the role of the aberrations of the optical system in interferometry we assume that surfaces d and b do not introduce any distortion into the reflecting and transmitting waves. This means that the surfaces under consideration are exactly plane and parallel (Fig. 1a) or exactly spherical and concentric (Fig. 1b). Moreover, besides the difference related to the aberrations, the waves propagate normally to the surfaces. Our approach allows the consideration of a more general case with tilted and distorted surfaces, but the analysis becomes considerably more complex. For example, the propagation of the wave reflected from the surface b must be considered step by step (from the surface d to the surface b and in the opposite direction), the same distortion of the surface d for the first wave has a reflecting character and for the second wave – refracting one, etc. The main aim of the paper is the estimation of the influence of the optical aberrations and nonuniform illumination only.

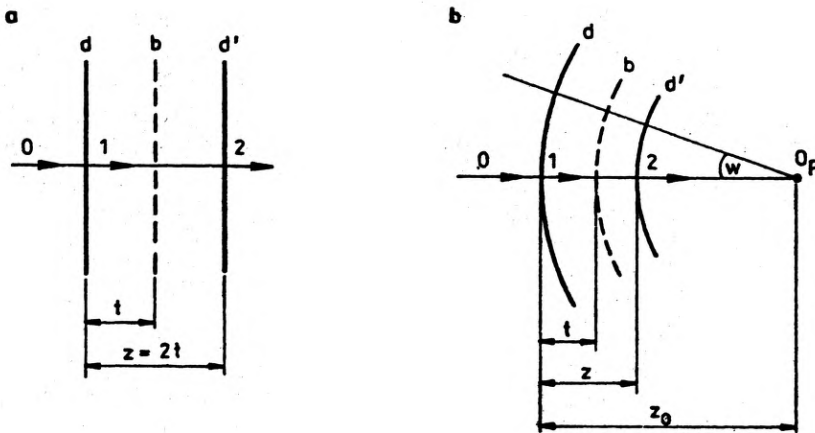


Fig. 2. Evolution of the wave propagation in interferometers with the reflection (Fig. 1) into the one direction wave propagation for plane (a) and spherical (b) surfaces

To simplify our consideration we unfold the system with the reflections (see Fig. 1a) into the system with one direction of the wave propagation (see Fig. 2a). The arrows and the numbers marked in Fig. 1 and 2 concern the same states of the waves. This means that the original wave 0 (fig. 2a) generates waves 1 and 2, and wave 1 determined in the plane d interferes with wave 2 determined in the plane d' . The state of wave 2 in the plane d' is derived from the state of wave 1 in the plane d by analysing the propagation of the original wave between the planes d and d' . The difference between the phase distributions on the planes d' and d described in linear coordinates determines the interferometer error introduced by the propagation of the original wave. Only for the plane wave case the mentioned error equals zero. Any aberration or variable amplitude distribution of the original wave induces some phase difference which has to be estimated.

A similar unfolding can be performed for the system with spherical elements (see Figs. 1b and 2b). However, in this case the wave propagation must be described in the angular coordinates defined from the centre of the curvature O_F of the spherical surfaces (angle w in Fig. 2b). The equivalent distance z between the surfaces d and d' is given by the equation (see Appendix 1)

$$z = \frac{2t}{1 + \frac{t}{z_0}} \quad (1)$$

where z_0 designates the radius of curvature of surface d of the reference plate standard. For $z_0 \rightarrow \infty$, we have $z = 2t$ (see, for comparison, Fig. 2a).

To analyse the interference of waves 1 and 2 generated by the original aberrated wave 0 and reflected by the spherical surfaces d and b (see Fig. 1b), it is sufficient to determine the difference between the phase distributions on the spheres d and d' . Both distributions are compared according to the geometrical shadow principle, as seen from the common centre of curvature O_F . The field distribution on the sphere d' is the result of propagation of the field distribution from the sphere d .

The proposed unfolding of the system with reflecting surfaces (Fig. 1) into the equivalent sets shown in Fig. 2 simplifies our consideration essentially. It reduces to the analysis of the field propagation between the concentric spheres d and d' (Fig. 2b) or between the parallel planes d and d' (Fig. 2a). It is worth to remark that the case with the spherical elements is more general, and the case with the planar elements can be reached by putting $z_0 \rightarrow \infty$.

3. Solution of the problem

Let $V(\bar{a})$ be a field distribution on a sphere Σ and the problem is to find the field distribution $V'(\bar{a}')$ on a sphere Σ' as a propagation result of the distribution $V(\bar{a})$ (Fig. 3). The centres of both spheres coincide and let point O_F be the point of coincidence. According to Fig. 3, the Fourier transform of $V(\bar{a})$ arises on the sphere Σ_F with the centre at O . The field distribution $V_F(\bar{\rho})$ on the sphere Σ_F can be found

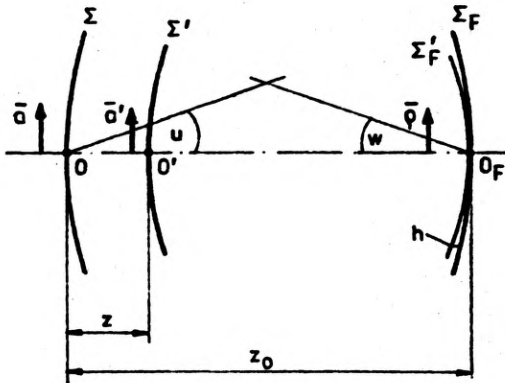


Fig. 3. Determination of the wave propagation between the concentric spheres Σ and Σ' with the aid of changes of Fourier distributions between the spheres Σ_F and Σ'_F .

from the expression

$$V_F(\bar{\rho}) = \frac{1}{\lambda z_o} \iint V(\bar{a}) \exp\left(-i \frac{k\bar{\rho}\bar{a}}{z_o}\right) d\bar{a}, \tag{2}$$

$\bar{\rho}$, \bar{a} – radial position vectors on the spheres Σ_F and Σ , respectively, $d\bar{a}$ – elementary area of the sphere Σ , $k = 2\pi/\lambda$, λ – light wavelength.

To find the distribution $V'(\bar{a}')$ on sphere Σ' we shall find first the field distribution $V'_F(\bar{\rho})$ on sphere Σ'_F with the centre at O' . According to Fig. 3, we have

$$V'_F(\bar{\rho}) = V_F(\bar{\rho}) \exp(-ikh) \tag{3}$$

where h is the distance between the spheres Σ_F and Σ'_F measured in the axial direction, i.e.

$$h = \frac{\rho^2}{2} \left(\frac{1}{z_o - z} - \frac{1}{z_o} \right). \tag{4}$$

Now, for field distribution $V'(\bar{a}')$ we have

$$V'(\bar{a}') = \frac{1}{\lambda(z_o - z)} \iint V'_F(\bar{\rho}) \exp\left(i \frac{k\bar{\rho}\bar{a}'}{z_o - z}\right) d\bar{\rho} \tag{5}$$

where \bar{a}' – the radial vector on sphere Σ' . Eqs. (2)–(5) are valid for systems with small angles u and w (Fig. 3), and for $|z/r_o| \ll 1$ (for details, see [8], [9]). The maximum values of u , w and $|z/r_o|$ depend on the precision required.

Formulae (2) and (5) form the base to compute the demanded distribution $V'(\bar{a}')$. The method requires the application of two Fourier transformations, the first one to find field distribution $V_F(\bar{\rho})$ with the aid of distribution $V(\bar{a})$ (see Eq. (2)), and the second one to find field distribution $V'(\bar{a}')$ using field distribution $V'_F(\bar{\rho})$ (see Eq. (5)). Equations (3) with (4) give the relation between distributions $V'_F(\bar{\rho})$ and $V_F(\bar{\rho})$. We propose to reduce the integral relations (2) and (5) to one relation in a differential form.

First we introduce dimensionless coordinates:

$$\bar{a}_n = \frac{\bar{a}}{a_m}, \tag{6a}$$

$$\bar{\rho}_n = \frac{ka_m}{z_o} \bar{\rho} \tag{6b}$$

where a_m is an arbitrary dimension on sphere Σ .

It the field distribution $V(\bar{a})$ on sphere Σ is limited, then $2a_m$ may equal, for example, the maximum dimension of the area with this distribution. The return to the linear coordinates is obtained by putting $a_m = 1$ only. The quantity $\bar{\rho}_n$ is the parametrized angular coordinate of points on the spheres Σ_F and Σ'_F as seen from the point O . The vectorial form of the coordinate indicates the positions of the points in different meridional sections.

The notations adopted are convenient because the quantities used are dimensionless. Moreover, the values of the parameters can be compared to then known results. For example, if the field distribution $V(\bar{a})$ is constant in the circular area with the diameter $2a_m$ ($V(\bar{a}) = 0$ outside this area), then $a_{n,\max} = 1$ and the value $\rho_n = 3.83\dots$ relates to the half-diameter of the central part of the Airy disc.

Because according to (6) $d\bar{a} = a_m^2 d\bar{a}_n$ and $d\bar{\rho} = z_o^2 / (k^2 a_m^2) d\bar{\rho}_n$, then in place of Eqs. (2), (3) and (5) one can write:

$$R_F(\bar{\rho}_n) = \iint V(\bar{a}_n) \exp(-i\bar{a}_n \bar{\rho}_n) d\bar{a}_n, \quad (7)$$

$$R'_F(\bar{\rho}_n) = R_F(\bar{\rho}_n) \exp(-iZ\rho_n^2), \quad (8)$$

$$V'(\bar{a}'_n) = \frac{z_o}{z_o - z} \frac{1}{4\pi^2} \iint R'_F(\bar{\rho}_n) \exp(i\bar{a}'_n \bar{\rho}_n) d\bar{\rho}_n \quad (9)$$

where

$$R_F(\bar{\rho}_n) = z_o V_F(\bar{\rho}_n) \frac{\lambda}{a_m^2}, \quad (10a)$$

$$R'_F(\bar{\rho}_n) = z_o V'_F(\bar{\rho}_n) \frac{\lambda}{a_m^2}. \quad (10b)$$

Because V_F and V'_F are the surface field distributions, then the quantities $V_F V_F^*$ and $V'_F V'^*_F$ (where the asterisk denotes the conjugate quantity) are proportional to the surface energy density of the propagated wave related to the elementary area of the spheres Σ_F and Σ'_F , respectively (see [10] Sect. 1.4, for comparison). For the same reason the quantities $z_o^2 V_F V_F^*$ and $z_o^2 V'_F V'^*_F$ are proportional to the angular energy density related to the elementary solid angle defined from the point O . This means that according to Eqs. (10) the quantities $R_F(\bar{\rho}_n)$ and $R'_F(\bar{\rho}_n)$ are the parametrized angular distributions $V_F(\bar{\rho}_n)$ and $V'_F(\bar{\rho}_n)$ for different values of distance z_o with the case $z_o \rightarrow \infty$ included. So, the notations introduced have allowed us to establish the relations (7)–(9) valid for an arbitrary large distance z_o .

The dimensionless parameter

$$Z = \frac{\lambda z}{4\pi a_m^2 \left(1 - \frac{z}{z_o}\right)} \quad (11)$$

is a measure of distance z between the spheres Σ' and Σ (see Fig. 3), which in the special case $z_o \rightarrow \infty$ become the planes (see for comparison Figs. 2b and 2a).

The normalized position vector \bar{a}'_n on sphere Σ' is given by

$$\bar{a}'_n = \bar{a}' / a'_m \quad (12)$$

where the quantity a'_m is a dimension on the sphere Σ' defined as the geometrical shadow of a_m as seen from the centre $O_{F'}$, i.e.

$$a'_m = a_m \frac{z_o - z}{z_o}. \quad (13)$$

Using the power series expansion

$$\exp(-iZ\rho_n^2) = 1 + \sum_{s=1}^M \frac{(-iZ)^s}{s!} \rho_n^{2s}, \tag{14}$$

and substituting Eq. (8) into Eq. (9), we can write

$$V'(\vec{a}'_n) = \frac{z_o}{z_o - z} \left[\frac{1}{4\pi^2} \iint R_F(\vec{\rho}_n) \exp(i\vec{a}'_n \vec{\rho}_n) d\vec{\rho}_n + \sum_{s=1}^M \frac{(-iZ)^s}{s!} \frac{1}{4\pi^2} \iint R_F(\vec{\rho}_n) \rho_n^{2s} \exp(i\vec{a}'_n \vec{\rho}_n) d\vec{\rho}_n \right]. \tag{15}$$

Such a way of analysis is justified, because according to (11), for partial cases, the value of Z is very small with comparison to 1 (for $z_{\max} < 2a_m$ and $a_m = 50$ mm the quantity Z is less than 10^{-5}). Moreover, if the Fourier field distribution is concentrated (the maximum value of ρ_n is assumed to be limited), then it will be sufficient to use the term with $s = 1$, only. Using Eq. (7) we can write

$$V'(\vec{a}'_n) = \frac{z_o}{z_o - z} [V(\vec{a}'_n) + \Delta V(\vec{a}'_n)] \tag{16}$$

where

$$\Delta V(\vec{a}'_n) = \sum_{s=1}^M \frac{(-iZ)^s}{s!} \frac{1}{4\pi^2} \iint R_F(\vec{\rho}_n) \rho_n^{2s} \exp(i\vec{a}'_n \vec{\rho}_n) d\vec{\rho}_n. \tag{17}$$

Now we can conclude that the field distribution $V'(\vec{a}'_n)$ on the sphere Σ' can be determined as the sum of the field distribution $V(\vec{a}'_n)$ from the sphere Σ and its change $\Delta V(\vec{a}'_n)$. All three quantities $V(\vec{a}'_n)$, $V'(\vec{a}'_n)$ and $\Delta V(\vec{a}'_n)$ relate to the vector coordinate \vec{a}'_n which according to (12) and (13) is defined as a geometrical shadow of the vector \vec{a}_n as seen from the point O_F (Fig. 3). The field change $\Delta V(\vec{a}'_n)$, according to (17), is equal to a sum of terms which are proportional to the inverse Fourier transform of respective moments of the angular Fourier transform distribution $R_F(\vec{\rho}_n)$. The coefficient $z_o/(z_o - z)$ in Eq. (16) relates to the photometric law of the wave amplitude changes. Namely, it gives the amplitude changes of a spherical wave with the centre at O_F during the propagation between the spheres Σ and Σ' . The reason of the appearance of this coefficient is the application of the equivalence set of the optical system (see Fig. 2b). In the real optical system (see Fig. 1b), we have to do with both the convergent and divergent spherical waves and this coefficient disappears.

Let ρ_{nx} , ρ_{ny} and a'_{nx} , a'_{ny} be the Cartesian components of the vectors $\vec{\rho}_n$ and \vec{a}'_n , respectively. Since $\vec{a}'_n \vec{\rho}_n = a'_{nx} \rho_{nx} + a'_{ny} \rho_{ny}$, and according to Eq. (7)

$$V(\vec{a}'_n) = \frac{1}{4\pi^2} \iint R_F(\vec{\rho}_n) \exp(i\vec{a}'_n \vec{\rho}_n) d\vec{\rho}_n, \tag{18}$$

then, if function $V(\vec{a}'_n)$ is differentiable α times with respect to a'_{nx} and β times with respect to a'_{ny} , we can write [11]

$$\frac{\partial^{(\alpha+\beta)} V(\vec{a}'_n)}{\partial a'^{\alpha}_{nx} \partial a'^{\beta}_{ny}} = i^{\alpha+\beta} \frac{1}{4\pi^2} \iint R_F(\vec{\rho}_n) \rho_{nx}^{\alpha} \rho_{ny}^{\beta} \exp(i\vec{a}'_n \vec{\rho}_n) d\vec{\rho}_n. \tag{19}$$

Because

$$\rho_n^{2s} = (\rho_{nx}^2 + \rho_{ny}^2)^s = \sum_{j=0}^s \binom{s}{j} \rho_{nx}^{2(s-j)} \rho_{ny}^{2j} \quad (20)$$

where $\binom{s}{j} = \frac{s!}{j!(s-j)!}$, then in place of (17) we have

$$\Delta V(\vec{a}_n) = \sum_{s=1}^M \frac{(iZ)^s}{s!} \left[\sum_{j=0}^s \binom{s}{j} \frac{\partial^{(2s)} V(\vec{a}_n)}{\partial a_{nx}^{(2s-2j)} \partial a_{ny}^{(2j)}} \right], \quad (21)$$

and, according to (16), finally

$$V'(\vec{a}'_n) = \frac{z_0}{z_0 - z} \left\{ V(\vec{a}_n) + \sum_{s=1}^M \frac{(iZ)^s}{s!} \left[\sum_{j=0}^s \binom{s}{j} \frac{\partial^{(2s)} V(\vec{a}_n)}{\partial a_{nx}^{(2s-2j)} \partial a_{ny}^{(2j)}} \right] \right\}. \quad (22)$$

Equation (22) is the demanded form of the relation allowing the determination of the field distribution $V'(\vec{a}'_n)$ on sphere Σ' with the aid of the field distribution $V(\vec{a}_n)$ from sphere Σ (Fig. 3). According to (11) parameter Z is a dimensionless measure of

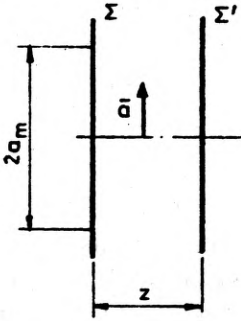


Fig. 4. Determination of the wave propagation between the planes Σ and Σ'

the distance z between the spheres Σ and Σ' . The field distribution $V(\vec{a}'_n)$, as a function of the vector position \vec{a}'_n on sphere Σ' , is taken as the geometrical shadow of the field distribution $V(\vec{a}_n)$ from sphere Σ , as seen from the point O_F . The formula (22) is valid for functions $V(\vec{a}_n)$ differentiable M times with respect to the components a_{nx} and a_{ny} of the vector \vec{a}_n . It means, in particular, that the method proposed can not be used for the analyses of the field truncated by a diaphragm. Partially we can consider the field sufficiently far from its geometrical shadow, where the influence of the diaphragm can be taken as negligibly small [12], Chapt. 6.

For $M = 2$ according to (22) we have

$$V'(\vec{a}'_n) = \frac{z_0}{z_0 - z} \left[V(\vec{a}_n) + iZ \left(\frac{\partial^2 V}{\partial a_{nx}^2} + \frac{\partial^2 V}{\partial a_{ny}^2} \right) - \frac{Z^2}{2} \left(\frac{\partial^4 V}{\partial a_{nx}^4} + 2 \frac{\partial^4 V}{\partial a_{nx}^2 \partial a_{ny}^2} + \frac{\partial^4 V}{\partial a_{ny}^4} \right) \right]. \quad (23)$$

As we have shown (see remark after Eq. (15)), in our case the quantity Z is very small. Then, for fields with small changes on the sphere Σ (small values of their derivatives) the term with Z^2 can be omitted.

For a field distribution $V(a)$ with rotational symmetry, we can write in place of Eq. (23)

$$V'(a'_n) = \frac{z_o}{z_o - z} \left[V(a'_n) + iZ \left(\frac{\partial^2 V}{\partial a_n'^2} + \frac{1}{a'_n} \frac{\partial V}{\partial a'_n} \right) - \frac{Z^2}{2} \left(\frac{\partial^4 V}{\partial a_n'^4} + \frac{2}{a'_n} \frac{\partial^3 V}{\partial a_n'^3} - \frac{1}{a_n'^2} \frac{\partial^2 V}{\partial a_n'^2} + \frac{1}{a_n'^3} \frac{\partial V}{\partial a'_n} \right) \right]. \tag{24}$$

Field distribution on a plane

As it was mentioned before, Equation (22) with auxiliary relations (11) and (13) is valid for the case $z_o \rightarrow \infty$ (Fig. 4). This conclusion concerns Eqs. (23) and (24), as well. For $z_o \rightarrow \infty$ the form of equations will be simpler, because the coefficient $z_o/(z_o - z) = 1$ and according to (13), (6a) and (12) one can use the same position vector \bar{a} (or \bar{a}_n) for both planes Σ and Σ' .

Remarks

The obtained results are in agreement with the solution of the paraxial-wave equation [13], but for the first term ($M = 1$) in the sum only. We have proved (see Appendix 2) that besides this first term the second one in our expression for the rotational symmetry case (Eq. (24)) is in full agreement with the results of the analysis of the defocused image of the point. These results were obtained on the base of Lommel functions. Moreover, our approach allows the analysis of the propagation of fields defined on spheres, not only on planes. The analysis of cases with sharp changes of the fields, because of infinitely large values of the derivatives, can not be conducted by our method.

4. Influence of the illumination nonuniformity

If $V(\bar{a})$ is a field distribution on the sphere Σ (Fig. 3), then according to the formulae (23) and (24) the field distribution $V(\bar{a}'_n)$ on the sphere Σ' can be found from the expression

$$V'(\bar{a}'_n) = \frac{z_o}{z_o - z} [V(\bar{a}'_n) + i\Delta V_i(\bar{a}'_n)] \tag{25}$$

where

$$\Delta V_i(\bar{a}'_n) = Z \left(\frac{\partial^2 V}{\partial a_{nx}'^2} + \frac{\partial^2 V}{\partial a_{ny}'^2} \right), \tag{26a}$$

and for the rotational symmetry case

$$\Delta V_i(a'_n) = Z \left(\frac{\partial^2 V}{\partial a_n'^2} + \frac{1}{a'_n} \frac{\partial V}{\partial a'_n} \right). \tag{26b}$$

Because the quantity $V(\vec{a}_n)$ is real (the interferometric optical system free of aberrations), then $\Delta V_i(\vec{a}_n)$ is also real. Moreover in practical cases, the values of $\Delta V_i(\vec{a}_n)$ are small with comparison to $V(\vec{a}_n)$. If we put

$$V'(\vec{a}'_n) = |V'(\vec{a}'_n)| \exp[2\pi i W(\vec{a}'_n)], \quad (27)$$

then

$$W(\vec{a}'_n) = \frac{\Delta V_i(\vec{a}'_n)}{2\pi V(\vec{a}'_n)}. \quad (28)$$

The fractional quantity $W = \Delta l / \lambda$ represents the measurement error in an interferometric system introduced by the nonuniform illumination, where Δl is the optical path error introduced. In other words, the quantity W is the aberration of the propagating beam induced by its variable amplitudes distribution.

The changed intensity distribution $I'(\vec{a}'_n)$ of the propagating wave can also be given in the form $I'(\vec{a}'_n) = |V'(\vec{a}'_n)|^2 = I(\vec{a}'_n) + \Delta I(\vec{a}'_n)$, but the change of the intensity distribution $\Delta I(\vec{a}'_n)$ is too small to influence the interferometric measurements.

Gaussian beam

Let in the plane Σ (Fig. 4) be given a field distribution in the form

$$V(a) = V_o \exp \left[- \left(\frac{a}{\omega_o} \right)^2 \right], \quad (29)$$

V_o and ω_o are constants.

We have taken the case of the Gaussian beam as an example of a typical nonuniform illumination. Moreover, there is an analytical solution of the Gaussian beam propagation [7]. To simplify the calculations the waist of the Gaussian beam is assumed at the plane Σ . $2\omega_o$ is the waist diameter. If we admit an arbitrary dimension in the plane Σ as $2a_m = 2\omega_o$ then

$$V(a_n) = V_o \exp(-a_n^2). \quad (30)$$

According to (26b) and (11), because $z_o \rightarrow \infty$, we have

$$\Delta V_i(a_n) = \frac{\lambda z}{\pi a_m^2} (a_n^2 - 1) V(a_n),$$

and from (28), because $a_m = \omega_o$

$$W = \frac{\lambda z}{2\pi^2 \omega_o^2} \left[\left(\frac{a}{\omega_o} \right)^2 - 1 \right]. \quad (31)$$

The phase changes of the Gaussian beam known from the analytical solution are given by [7]

$$W = \frac{1}{2\pi} \left(\phi + \frac{ka^2}{2R} \right) \quad (32)$$

where

$$R = -z \left[1 + \left(\frac{D}{2z} \right)^2 \right]$$

is the radius of the curvature of the wavefront Σ' at a distance z from the beam waist (see Fig. 5) ($D = k\omega_0^2$ is the confocal parameter of the Gaussian beam). Because $\tan\phi = 2z/D$ and $|z| \ll D$, then $\phi \approx 2z/D$ and $R = -D^2/(4z)$. After substituting the last relations into (32), we will obtain the relation (31). So, we have shown that the results obtained by our method and from the Gaussian beam equation are identical.

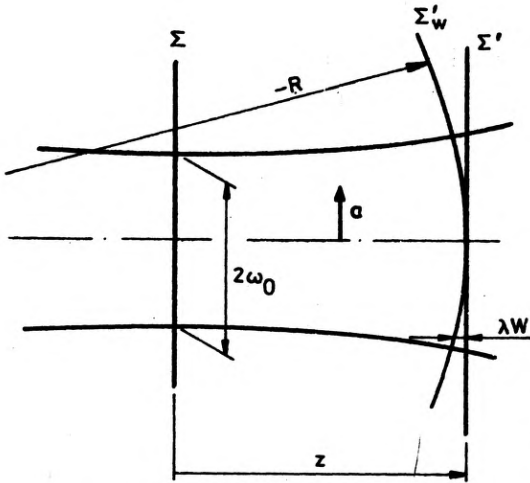


Fig. 5. Propagation of Gaussian beam between the planes Σ and Σ' . Σ'_w is a wavefront related to the plane Σ'

The constant phase corrections in interferometric measurements are not essential and they can be omitted. Therefore, according to (31) the measurement error introduced by the Gaussian character of the illumination is given by the expression

$$W = \frac{\lambda z a^2}{2\pi^2 \omega_0^4} \tag{33}$$

The maximum error occurs at the edge of the field of view (for a_{\max}). Usually the diameter of the Gaussian beam waist is greater than the diameter of the field of view of the interferometer ($\omega_0 > a_{\max}$). Moreover, the maximum distance z is of order of the diameter of the field ($z_{\max} \approx 2a_{\max}$). So, on the account of (33) error W is of order of 10^{-5} or less and it can be neglected.

Local amplitude changes on a spherical wavefront

Let

$$V(a) = V_o - V_a \exp \left[- \left(\frac{a}{\omega_o} \right)^2 \right] \tag{34}$$

be an amplitude distribution defined on the sphere Σ (Fig. 3). The quantities V_o , V_a , and ω_o are real and positive, moreover $V_a < V_o$. The field distribution defined by (34) represents the spherical wave of amplitude V_o with a local axial absorption. The character of absorption is Gaussian and the value of ω_o indicates the dimension of

the area of the area with its significant value. Using the dimensionless coordinates according to (6a), we have

$$V(a_n) = V_o - V_a \exp \left[- \left(\frac{a_n}{\omega_{no}} \right)^2 \right] \tag{35}$$

where $\omega_{no} = \omega_o/a_m$. $2a_m$ is the diameter of the field of view of an interferometer.

The field distribution on the sphere Σ' (Fig. 3) can be found from (25), where according to (26b) and (34)

$$\Delta V_i(a'_n) = Z \frac{4V_a}{\omega_{no}^2} \left[1 - \left(\frac{a'_n}{\omega_{no}} \right)^2 \right] \exp \left[- \left(\frac{a'_n}{\omega_{no}} \right)^2 \right].$$

Making use of (11), returning to the quantities ω_o and a' , and using (28), the measurement error can be described by the following expression:

$$W = W_o B (1 - \gamma^2) \exp(-\gamma^2) \tag{36}$$

where

$$W_o = \frac{1}{2\pi^2 \left(1 - \frac{z}{z_o} \right)} \frac{\lambda z}{\omega_o^2} \frac{V_a}{V_o - V_a} \tag{37}$$

is the value of W for $a = 0$, and

$$B = \frac{V_o - V_a}{V_o - V_a \exp(-\gamma^2)}, \tag{38a}$$

$$\gamma = \frac{a'}{\omega_o}. \tag{38b}$$

The quantity B fulfills the relation $0 < B \leq 1$, but for the small value of V_a with comparison to V_o we have $B \approx 1$. The diagram of the changes of W in the area of a local absorption is given in Fig. 6. The maximum error $W_{max} = W_o$ occurs in the centre of this area. If we assume that the changes of B are small, then for the minima we have $\gamma_1^2 = 2$ and $W_1 = -0.135 W_o B$. According to (37) the maximum error W_o increases with an increase of distance z of the wave propagation and the absorption

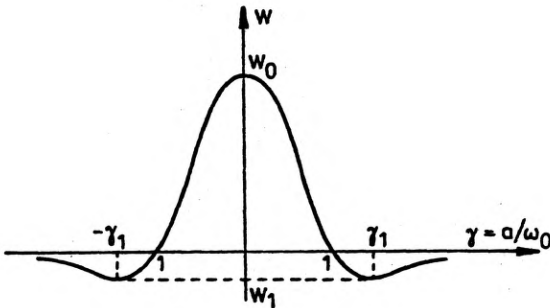


Fig. 6. Distribution of measurement error W in the test field of an interferometer in the case of Gaussian local amplitude absorption

degree V_a/V_o , and with the decrease of the dimension $2\omega_o$ of a local absorption. This error can take significant values for large distances z and small dimension $2\omega_o$, when the value of ω_o^2 is comparable to the value of λz .

Remarks

For the propagation of a whole Gaussian beam, then maximum aberration occurs as the edge of the field of view, but for the spherical (or plane) wave with a local Gaussian change of the amplitude – in the centre of this local area. These facts are not contradictory. The apparent difference relates to the constant phase correction ϕ characteristic for the Gaussian beam (see Eq. (31)). For the interferometric measurements, the constant phase shift is of no importance. However, the shift between the spherical (or plane) wave and its local Gaussian disturbance is the reason of the interferometric error introduced by the local Gaussian absorption.

In the case of a strong local absorption Equation (37) fails ($V_a \rightarrow V_o$ and $W_o \rightarrow \infty$), and it is necessary to use the relation $\tan(2\pi W) = \Delta V_r(\vec{a}_n)/V(\vec{a}_n)$ in place of (28).

5. Changes of wave aberrations during the wavefront propagation

Let

$$V(\vec{a}_n) = V_o \exp[2\pi i W(\vec{a}_n)] \tag{39}$$

be the field distribution on the sphere Σ (Fig. 3) with a constant amplitude V_o and a variable aberration $W(\vec{a}_n)$. According to (23) for $M = 1$ and (39), we can write

$$V'(\vec{a}'_n) = \frac{z_o}{z_o - z} V(\vec{a}'_n) [1 + \Delta v_r(\vec{a}'_n) + i \Delta v_i(\vec{a}'_n)] \tag{40}$$

where:

$$\Delta v_r(\vec{a}'_n) = -2\pi Z \left(\frac{\partial^2 W}{\partial a'^2_{xn}} + \frac{\partial^2 W}{\partial a'^2_{yn}} \right), \tag{41a}$$

$$\Delta v_i(\vec{a}'_n) = -4\pi^2 Z \left[\left(\frac{\partial W}{\partial a'_{xn}} \right)^2 + \left(\frac{\partial W}{\partial a'_{yn}} \right)^2 \right]. \tag{41b}$$

Putting $V'(\vec{a}'_n) = |V'(\vec{a}'_n)| \exp[2\pi i W'(\vec{a}'_n)]$ and assuming that the wave aberration $W(\vec{a}_n)$ is not large, the quantities $\Delta v_r(\vec{a}'_n)$ and $\Delta v_i(\vec{a}'_n)$ are sufficiently small to write

$$W'(\vec{a}'_n) - W(\vec{a}'_n) \approx \frac{1}{2\pi} \frac{\Delta v_i(\vec{a}'_n)}{1 + \Delta v_r(\vec{a}'_n)} \approx \frac{1}{2\pi} \Delta v_i(\vec{a}'_n), \tag{42}$$

and on account of (11) and (41b) we get

$$\Delta W(\vec{a}'_n) = - \frac{z\lambda}{2 \left(1 - \frac{z}{z_o}\right) a_m^2} \left[\left(\frac{\partial W}{\partial a'_{xn}} \right)^2 + \left(\frac{\partial W}{\partial a'_{yn}} \right)^2 \right] \tag{43}$$

where $\Delta W(\vec{a}_n) = W'(\vec{a}_n) - W(\vec{a}_n)$. This is the demanded expression describing the interferometric error introduced by the propagation of the aberrated wave. The error $\Delta W(\vec{a}_n)$ is given as a fraction of λ .

Because the derivatives $\partial W/\partial a'_n$ relate to the angles of deviation of the optical rays, then the interferometric error $\Delta W(\vec{a}_n)$ can be described with the aid of the angular aberrations of the optical system (see Appendix 3, see for comparison [5]).

On account of Equation (40) one can determine the change of the intensity distribution induced by the propagation of the aberrated wave. This problem is out of scope of this paper.

Influence of the primary aberrations

Let us express the wave aberrations of the optical system of an interferometer according to the notation of HOPKINS [14] as

$$W(a_n, \theta) = W_{11}a_n \cos(\theta - \theta_{11}) + W_{20}a_n^2 + W_{40}a_n^4 + W_{31}a_n^3 \cos(\theta - \theta_{31}) + W_{22}a_n^2 \cos^2(\theta - \theta_{22}) \quad (44)$$

where $a_n = a/a_o$ and θ are the normalized polar coordinates in the field of view of an interferometer (Fig. 7). The quantities W_{11} (tilt of the wave surface), W_{20} (defocusing), W_{40} (spherical aberration), W_{31} (coma), W_{22} (astigmatism), similarly as the aberration function $W(a_n, \theta)$, are expressed as the fraction of λ . For $0 < a < a_o$ we have $0 \leq a_n < 1$. Usually the illuminating beam in the interferometer is axial and from the theoretical point of view the aberration function should have rotational symmetry.

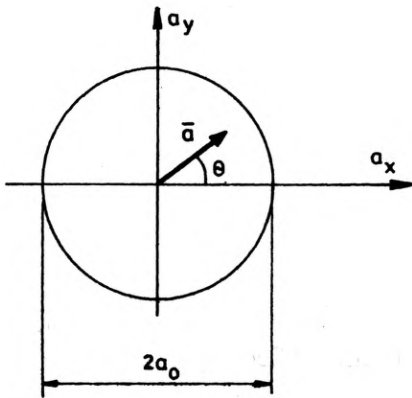


Fig. 7. Coordinates in the test field of an interferometer

The astigmatism can be introduced by a semitransparent plate located in a convergent beam and a defect of the objective mounting generates the coma aberration. The changes of the tilt coefficient W_{11} and defocusing W_{20} concern the adjustment of the interferometer. The azimuthal angles θ_{11} , θ_{31} and θ_{22} of the primary aberrations are independent. We do not lose generality if we assume that $\theta_{11} = 0$. This means that the inclination of the wavefront surface occurs in the meridional section coincident with the axis a_x (see Fig.7).

Using the relations: $a_{xn} = a_n \cos\theta$, $a_{yn} = a_n \sin\theta$ and $\cos(\theta - \theta_i) = \cos\theta \cos\theta_i + \sin\theta \sin\theta_i$ we can write from (44)

$$\begin{aligned} \frac{\partial W}{\partial a_{xn}} &= W_{11} + 2a_n \cos\theta (W_{20} + 2W_{40} a_n^2) \\ &+ W_{31} a_n^2 (2\cos\theta_{31} + 2\cos\theta_{31} \cos^2\theta + 2\sin\theta_{31} \sin\theta \cos\theta) \\ &+ W_{22} a_n (2\cos^2\theta_{22} \cos\theta + 2\sin\theta_{22} \cos\theta_{22} \sin\theta). \end{aligned}$$

The expression for $\partial W / \partial a_{yn}$ is similar, but we must interchange only all cosine and sine functions of the angles θ and θ_{ij} . Substituting the expression for $\partial W / \partial a_{xn}$ and $\partial W / \partial a_{yn}$ into (43), after rearranging the following equation is obtained

$$\Delta W(a'_n, \theta) = - \frac{\lambda z}{2a_o^2 \left(1 - \frac{z}{z_o}\right)^s} \sum_s T_s(a'_n, \theta). \tag{45}$$

It describes the interferometric error induced by the aberration wave defined in Eq. (44). The components $T_s(a'_n, \theta)$ of the sum in Equation (45) are grouped in two tables in different orders. Table 1 contains the components ordered with respect to the combinations of the primary aberrations, and Table 2 – with respect to the powers of a'_n . In both tables the term W_{11}^2 has been omitted as the constant phase factor. The different orders of both tables facilitate the formulation of different conclusions. Using the terms in Table 1 one can find easily the relations between the influences of different primary aberrations. Table 2 allows us to distinguish the influence of the primary aberrations in the different areas of the field of view. The terms with the higher powers of a'_n concern the areas situated nearer to the edge of the field of view.

Table 1. Set of components $T_s(a'_n, \theta)$ of the sum in Equation (45) ordered with respect to the combinations of the aberrations

s	Aberration combinations	Components $T_s(a'_n, \theta)$
1	Defocusing with spherical aberration alone (W_{sf})	$4W_{sf}^2$
2	Coma alone (W_{31})	$a_n^4 W_{31}^2 \left[1 + 8\cos(\theta - \theta_{31}) \right]$
3	Astigmatism alone (W_{22})	$4a_n^2 W_{22}^2 \cos^2(\theta - \theta_{22})$
4	Tilt and defocusing with spherical aberration (W_{11} and W_{sf})	$4W_{11} W_{sf} \cos\theta$
5	Tilt and coma (W_{11} and W_{31})	$2a_n^2 W_{11} W_{31} [\cos(2\theta - \theta_{31}) + 2\cos\theta_{31}]$
6	Tilt and astigmatism (W_{11} and W_{22})	$4a_n W_{11} W_{22} \cos\theta_{22} \cos(\theta - \theta_{22})$
7	Defocusing with spherical aberration and coma (W_{sf} and W_{31})	$12a_n^2 W_{sf} W_{31} \cos(\theta - \theta_{31})$
8	Defocusing with spherical aberration and astigmatism (W_{sf} and W_{22})	$8a_n W_{sf} W_{22} \cos^2(\theta - \theta_{22})$
9	Coma and astigmatism (W_{31} and W_{22})	$4a_n^3 W_{31} W_{22} \cos(\theta - \theta_{22}) \times [2\cos(\theta - \theta_{31})\cos(\theta - \theta_{22}) + \cos(\theta_{22} - \theta_{31})]$

Table 2. Set of components $T_s(a'_n, \theta)$ of the sum in Equation (45) ordered with respect to the powers of a'_n

s	Components $T_s(a'_n, \theta)$
1	$a'_n \{4W_{11} [W_{20} \cos \theta + W_{22} \cos \theta_{22} \cos(\theta - \theta_{22})]\}$
2	$a_n'^2 \{4W_{20}^2 + 4W_{22}^2 \cos^2(\theta - \theta_{22}) + 2W_{11} W_{31} [\cos(2\theta - \theta_{31}) + 2\cos \theta_{31}] + 8W_{20} W_{22} \cos^2(\theta - \theta_{22})\}$
3	$a_n'^3 \{8W_{11} W_{40} \cos \theta + 12W_{20} W_{31} \cos(\theta - \theta_{31}) + 4W_{31} W_{22} \cos(\theta - \theta_{22}) [2\cos(\theta - \theta_{31}) \cos(\theta - \theta_{22}) + \cos(\theta_{22} - \theta_{31})]\}$
4	$a_n'^4 \{16W_{20} W_{40} + W_{31}^2 [1 + 8\cos^2(\theta - \theta_{31})] + 16W_{40} W_{22} \cos^2(\theta - \theta_{22})\}$
5	$a_n'^5 24W_{40} W_{31} \cos(\theta - \theta_{31})$
6	$a_n'^6 16W_{40}^2$

For simplicity we have denoted

$$W_{sf} = a'_n (W_{20} + 2W_{40} a_n'^2). \quad (46)$$

For a given measurement accuracy one can determine admissible part ΔW_1 of the error introduced by the aberrations of the optical system. Depending on the construction of an interferometer, according to (45) and one of the tables, one can find the admissible values of the coefficient W_{ij} . As an example we will analyse the tolerances of the spherical aberration only. It means that we assume $W_{31} = W_{22} = 0$. In general, the coefficient $W_{11} \neq 0$. The beam axis should be perpendicular to the standard plane ($W_{11} = 0$) but, because of an adjustment error, this condition can not be fulfilled perfectly.

Tolerances of the spherical aberration

According to Equation (45) and Table 1 we have

$$\Delta W(a'_n, \theta) = - \frac{2\lambda z}{a_n'^2 \left(1 - \frac{z}{z_0}\right)} [W_{sf} (W_{sf} + W_{11} \cos \theta)]. \quad (47)$$

One can conclude that the tilt of the wavefront influences the interferometric error in the case $W_{sf} \neq 0$, only. This influence increases with the increase of $|W_{sf}|$. It means that we can assume a technically justified admissible value of W_{11} , and next determine the necessary correction.

The quantity W_{11} is the phase shift at the edge of the observation field expressed in λ . If a tilt angle is denoted by Φ , then

$$W_{11} = \frac{\Phi a_0}{\lambda} \quad (48)$$

where, as previously, $2a_0$ is the diameter of the observation field. For $\Phi = 30''$, $2a_0 = 200$ mm and $\lambda = 0.633 \times 10^{-3}$ mm we have $W_{11} = 23$. It signifies that the second term in the brackets of Eq. (47) has a main influence on the interferometric error. The influence of tilt can be comparable with the influence of spherical aberration alone if Φ is of order of $1''$. This condition is technically difficult to obtain. Because $0 \leq \theta < 2\pi$, then according to (47), the criterion of the aberration correction

can be formulated as follows:

$$|W_{sf}| \leq \frac{a_o^2 \left(1 - \frac{z}{z_o}\right) \Delta W_1}{2\lambda z W_{11,m}} \quad (49)$$

where ΔW_1 is a limit of admissible error in the whole field of view and $W_{11,m}$ – a maximum admissible value W_{11} .

If we assume, as previously, that the maximum distance z fulfills the relation $z_{\max} < 4a_o(1 - z/z_o)$ then

$$|W_{sf}(a'_n)| < \frac{a_o \Delta W_1}{8\lambda W_{11,m}}. \quad (50)$$

On account of (46), in place of (50) we have

$$|a'_n(W_{20} + 2W_{40}a_n'^2)| < \frac{a_o \Delta W_1}{8\lambda W_{11,m}}. \quad (51)$$

One of the possible solutions is the focused optical system ($W_{20} = 0$). Because the maximum error occurs at the edge of field ($a'_n = 1$), then the tolerance criterion of the spherical aberration takes the form

$$W_{40} < \frac{a_o \Delta W_1}{16\lambda W_{11,m}}. \quad (52)$$

For example, if the diameter of the field of view is $2a_o = 200$ mm, $\lambda = 0.633 \times 10^{-3}$ mm, $\Delta W_1 = 0.001$ (the maximum interferometric error $\lambda/1000$) and $W_{11,m} = 23$ ($\Phi = 30''$), then $|W_{40}| < 0.43$. One can decrease the requirement introducing some defocusing. According to (46) the extremum of function W_{sf} occurs for $a_{ne}'^2 = -W_{20}/(6W_{40})$. Comparing the values of the function ΔW for $a'_n = 1$ and $a'_n = a_{ne}'$ we obtain the optimization condition of the aberration correction in the form

$$W_{20} = -1.5 W_{40}, \quad (53)$$

and in place of (52) the aberration criterion becomes

$$W_{40} < \frac{a_o \Delta W_1}{4\lambda W_{11,m}}. \quad (54)$$

This means that the introduction of the defocusing according to (53) enlarges 4 times the tolerances (see relations (54) and (52), and also [1], for comparison). Some imperfection of this solution is the appearance of the maximum error also in the central part of the field (for $a'_n = 0.5$), not only at the edge of the field as in the case $W_{20} = 0$. Moreover, the problem of the proper adjustment (the fulfillment of condition (53)) is encountered.

Remarks

In order to analyse the influence of the amplitude and phase changes (the influence of the illumination nonuniformity and aberrations of the optical system) we have taken

into consideration first term ($s = 1$) of the sum in expansion (22), only. The second and further terms can be significant, if the distance of the wave propagation is considerably larger than the diameter of the field of view or the values of the derivatives of the higher orders are respectively large (the strong change of the amplitude and phase distribution of the propagating wave). Moreover, we have limited the phase analyses to the influence of the primary aberrations. In the same way one may take into account other phase changes. The analysis of the fifth order spherical aberrations is also particularly important, because it is possible to accomplish an optimization of the aberration correction without defocusing of the optical system, which facilitates its adjustment (paper in preparation).

6. Conclusions

We have proved that in the interferometric system with nonzero difference of the optical paths, the illumination nonuniformity and the aberrations of the optical system can have some effect upon the measurement accuracy. This effect is significant in the measurements with high accuracy and large differences of the optical paths. The sources of the interferometric errors are the changes of the wavefront upon its propagation. They are different on different optical paths.

From our considerations it results, in particular, that in the case of an admissible interferometric error $\lambda/1000$ and if the diameter of the Gaussian beam waist is greater than the diameter of the field of view of the interferometer, the change of amplitude introduced by the Gaussian beam illumination of an interferometer is not significant. But a strong local absorption with small diameter with comparison to the observation field diameter can introduce local phase changes influencing the interferometric error. The influence of the aberrations depends essentially on the wavefront tilt with regard to the standard surface. The requirements for the interferometer adjustment are technically difficult to fulfill. They can be decreased by the optimization of the aberration correction.

Appendix 1

Unfolding of the optical system of an interferometer

According to Figure 1b, let d and b (Fig. A.1.1) be the reflecting spheres with a common centre O_F . Let $V(\vec{a})$ be a complex field distribution generated on the surface d by the wave O . After the reflection the field distribution $V_1(\vec{a}) = rV^*(\vec{a})$ arises on the same surface, where r is the amplitude reflection coefficient of the reflecting surface and V^* - the conjugate quantity of V . Wave 2, after the

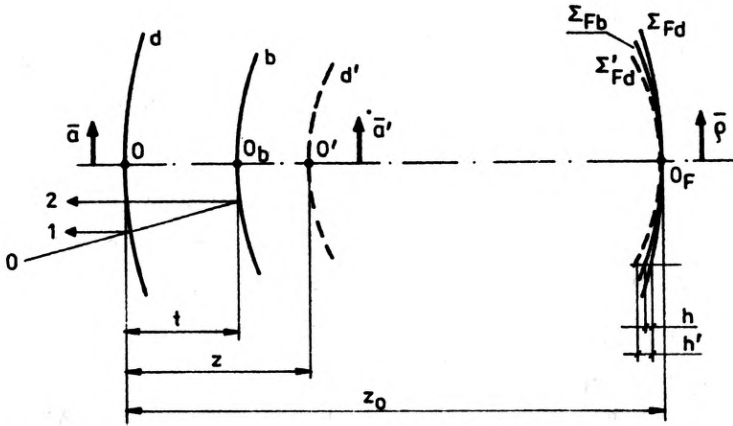


Fig. A.1.1. Determination of the wave propagation between concentric spheres with the aid of Fourier distributions on the spheres Σ_F

propagation between the surfaces d and b , the reflection on the surface b , the opposite propagation between the surfaces b and d and the transmission through the surface d , will produce the field distribution $V_2(\bar{a})$. The result of the interference is given by the sum

$$V_s(\bar{a}) = V_1(\bar{a}) + V_2(\bar{a}). \tag{A1.1}$$

We will prove that the same result can be obtained using in place of (A 1.1) the sum

$$V_s(\bar{A}) = V_1(\bar{A}) + V_2'(\bar{A}), \tag{A1.2}$$

for the parametrized coordinate

$$\bar{A} = \frac{k\bar{a}}{z_0} = \frac{k\bar{a}'}{z_0 - z} \tag{A1.3}$$

(see the notation in Fig. A1.1). V_1 is the same reflected field distribution on the surface d as in (A1.1), and V_2' is reflected field distribution on the sphere d' with the centre at O_F . Equations (A1.1) and (A1.2) will be equivalent, if relation (1) of the paper is fulfilled. In order to prove our thesis, it is sufficient to show that the field distribution $V_2(\bar{A})$ on sphere d equals the field distribution $V_2'(\bar{A})$ on sphere d' (the reflected field). To simplify our analysis, the equality of the field distributions will be replaced by the equality of their Fourier transforms. Moreover, we are interested in the phase distributions only. Therefore, we will neglect all reflection and transmission coefficients.

According to [15] and the notation (A1.3) we can write

$$V_F(\bar{\rho}) = C \text{FT}^- [V(\bar{A})] \tag{A1.4}$$

where FT^- – Fourier transform operator, $C = \lambda z_0 / (4\pi^2)$. The Fourier transform field distribution $V_F(\bar{\rho})$ arises on the reference sphere Σ_{Fd} with the centre at O (Fig. A1.1). The Fourier transform field distribution $V_{Fd}(\bar{\rho})$ related to the field distribution on

sphere b is given on sphere Σ_{Fb} with the centre at O_b and according to Fig. A.1.1

$$V_{Fd}(\bar{\rho}) = V_F(\bar{\rho})\exp(-ikh) \quad (\text{A1.5})$$

where

$$h = \frac{\rho^2}{2} \left(\frac{1}{z_o - t} - \frac{1}{z_o} \right). \quad (\text{A1.6})$$

The reflected field distribution on sphere b has also its own Fourier transform on sphere Σ_{Fb} , but its field distribution is described by the equation

$$V_{Fdr}(\bar{\rho}) = V_{Fd}^*(\bar{\rho}) = V_F^*(\bar{\rho})\exp(ikh). \quad (\text{A1.7})$$

The Fourier transform field distribution on sphere d for wave 2 propagating in the opposite direction arises on the sphere Σ_{Fd} and according to Fig. A1.1 and Eq. (A1.7) it will be

$$V_{Fr}(\bar{\rho}) = V_{Fdr}(\bar{\rho})\exp(ikh) = V_F^*(\bar{\rho})\exp(2ikh). \quad (\text{A1.8})$$

The Fourier transform field distribution $V'_{Fd}(\bar{\rho})$ related to the field distribution on the sphere d' arises on the sphere Σ'_{Fd} with the centre at O' , and in this case

$$V'_{Fd}(\bar{\rho}) = V_F(\bar{\rho})\exp(-ikh') \quad (\text{A1.9})$$

where according to Fig. A.1.1

$$h' = \frac{\rho^2}{2} \left(\frac{1}{z_o - z} - \frac{1}{z_o} \right). \quad (\text{A1.10})$$

After the reflection

$$V'_{Fd}(\bar{\rho}) = V_F^*(\bar{\rho})\exp(ikh). \quad (\text{A1.11})$$

The equality of the field distributions $V'_{Fd}(\bar{\rho})$, (Eq. (A1.11)), and $V_{Fdr}(\bar{\rho})$, (Eq. (A1.8)), is fulfilled when $h' = 2h$, which with the relations (A1.6) and (A1.10) gives the required relation (1) of the paper.

If a Fourier transform field distribution $V_{Fi}(\bar{\rho})$ on sphere Σ_{Fi} is known (Fig. A.1.2), then the field distribution $V_i(\bar{a}_i)$ on sphere Σ_i , according to (A1.1), is given by

$$V_i(\bar{A}) = \frac{1}{C_i} \text{FT}^+ [V_{Fi}(\bar{\rho})], \quad (\text{A1.12})$$

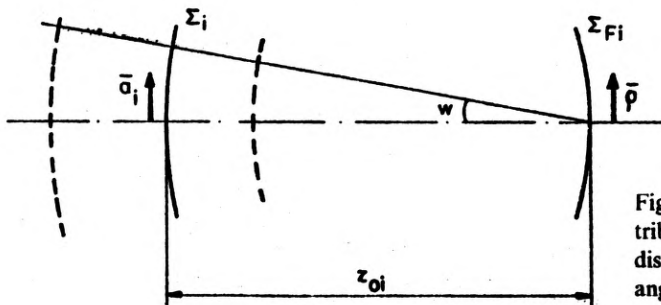


Fig. A.1.2. Relation between a field distribution on a sphere Σ_i and its Fourier distribution on a sphere Σ_{Fi} for the angular coordinate w

where FT^+ denotes the inverse Fourier transform operator, $C_i = \lambda z / (4\pi^2)$, $\bar{A} = k\bar{w}$, $\bar{w} = a_i / z_{oi}$. The centres of both spheres lie on each other. According to Fig. A1.2 the angle w , similarly as the parametrized vector coordinate \bar{A} , are common for all spheres Σ_i . Relation (A1.12) is fulfilled for different distances z_{oi} . This means that the equality of the Fourier transform field distributions for the different distances z_{oi} is equivalent to the equality of the field distributions on the different spheres Σ_i , but the last field distributions have to be described with the aid of the parametrized coordinate \bar{A} .

The analysis of the field propagation on the spheres with the aid of changes of the Fourier transforms was applied for the first time to analyse the Talbot effect [16].

Appendix 2

Airy beam

Let

$$V(a_n) = V_0 \frac{2J_1(a_n)}{a_n} \tag{A2.1}$$

be a field distribution on plane Σ (Fig. A.2) as the image of a point source given by an aberration free optical system. V_0 is the axial amplitude and

$$a_n = \frac{a}{a_0} \tag{A2.2}$$

where a is the radial coordinate. For simplicity, diameter $2a_0$ of the Airy pattern equals the radial distance between the points for which, according to (A2.1), the field amplitude decreases to $2J_1(1)$ of its axial value ($2J_1(1) \approx 0.8802$). Our problem is to find the field distribution in plane Σ' (Fig. A.2) at a distance z from plane Σ . We have mentioned before the Airy beam as an example to prove that our approach leads to the results obtained in the case of a defocused image point with the aid of Lommel functions.

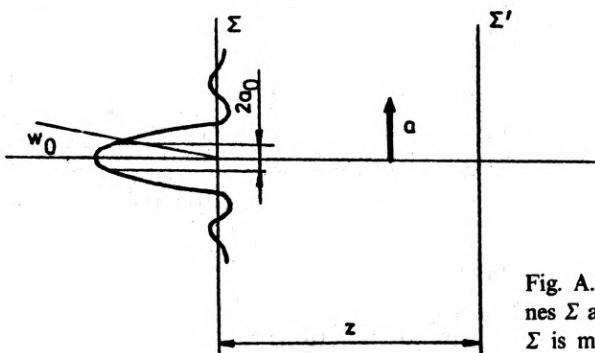


Fig. A.2. Propagation of Airy beam between planes Σ and Σ' . The field distribution on the sphere Σ is marked symbolically.

Because of the formulae (24), (A2.1), and the relation $\frac{\partial}{\partial x} [x^{-n} J_n(x)] = -x^n J_{n+1}(x)$ [17] we have:

$$\frac{\partial V}{\partial a_n} = -2V_0 a_n^{-1} J_2, \quad \frac{\partial^2 V}{\partial a_n^2} = -2V_0 \frac{\partial}{\partial a_n} [a_n(a_n^{-2} J_2)] = -2V_0(a_n^{-2} J_2 - a_n^{-1} J_3),$$

and

$$\frac{\partial^3 V}{\partial a_n^3} = 2V_0(3a_n^{-2} J_3 - a_n^{-1} J_4), \quad \frac{\partial^4 V}{\partial a_n^4} = 2V_0(3a_n^{-3} J_3 - 6a_n^{-2} J_4 + a_n^{-1} J_5).$$

For simplicity we have used the notation $J_n(a_n) = J_n$. Using the relation $J_{n+1}(x) = 2nJ_n(x)/x - J_{n-1}(x)$ for $n = 2$ and 4 [17], according to (24), (11) and (A2.1), for $z_0 \rightarrow \infty$, we get

$$V'(a_n) = V_0 \left\{ 2a_n^{-1} J_1 + \frac{i\lambda z}{2\pi a_0^2} (2a_n^{-2} J_2 - a_n^{-1} J_1) - \frac{1}{4} \left(\frac{\lambda z}{2\pi a_0^2} \right)^2 (8 - a_n^2) a_n^{-3} J_3 \right\}. \quad (\text{A2.3})$$

Applying the notation used in [10], Sect. 8.8, the field distribution in the defocused point image can be described by the formula

$$V'(u, v) = V_0 [C(u, v) - iS(u, v)] \quad (\text{A2.4})$$

where

$$C(u, v) = 2 \cos\left(\frac{u}{2}\right) \frac{U_1(u, v)}{u} + \text{sinc}\left(\frac{u}{2}\right) U_2(u, v), \quad (\text{A2.5})$$

$$S(u, v) = \text{sinc}\left(\frac{u}{2}\right) U_1(u, v) - 2 \cos\left(\frac{u}{2}\right) U_2(u, v), \quad (\text{A2.6})$$

and U_n is the Lommel function [10], Sect. 8.8,

$$U_n(u, v) = \sum_{s=0}^{\infty} (-1)^s \left(\frac{u}{v}\right)^{n+2s} J_{n+2s}(v) \quad (\text{A2.7})$$

($\text{sinc } x = \sin x / x$).

For the parametrized quantities u and v we have

$$u = kw_0^2 z = \frac{\lambda z}{2\pi a_0^2}, \quad (\text{A2.8})$$

$$v = kw_0 a = a_n, \quad (\text{A2.9})$$

because for the Airy pattern $kw_0 a_0 = 1$ (w_0 - aperture angle of the optical system generating the point image).

After substituting (A2.7) into (A2.6) and (A2.4), using the relations $\cos(u/2) = 1 - u^2/8 + \dots$, $\text{sinc}(u/2) = 1 - u^2/24 + \dots$, $J_3(x) = 4J_2(x)/x - J_1(x)$, and ordering the terms according to the powers of u , on account of (A2.8) and (A2.9), we obtain the relation (A2.3). This means that our formula (24) is in full agreement with the results obtained on the base of the Lommel functions.

Appendix 3

Angular aberrations

Let the phase distribution on reference sphere Σ with the centre at O_F (Fig.A.1.1) has the form

$$V(\vec{a}) = V_o \exp[2\pi i W(\vec{a})] \tag{A3.1}$$

where V_o is constant. According to [10], Sect. 5.1, the ray aberration computers can be found the expression

$$\Delta x = z_o \lambda \frac{\partial W}{\partial a_x}, \quad \Delta y = z_o \lambda \frac{\partial W}{\partial a_y}. \tag{A3.2}$$

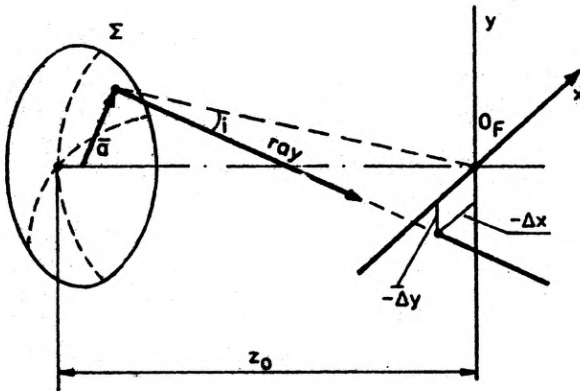


Fig. A.3. Relation between wave and geometrical aberrations defined on the sphere Σ and the plane x,y , respectively

The deviation angle $i(a')$ of the ray (see (A3.2) and Fig. A.3) is equal to

$$i^2(a') = \frac{\Delta x^2 + \Delta y^2}{z_o^2} = \lambda^2 \left[\left(\frac{\partial W}{\partial a_x} \right)^2 + \left(\frac{\partial W}{\partial a_y} \right)^2 \right], \tag{A3.3}$$

which with (6a) and (43) gives the following formula describing the interferometric error:

$$\Delta W(\vec{a}) = - \frac{i^2(\vec{a})z}{2\lambda \left(1 - \frac{z}{z_o} \right)}. \tag{A3.4}$$

This formula can be a basis for the geometrical analysis of the aberrations of the optical system of an interferometer (see [5], for comparison).

References

- [1] TAYLOR W. G. A., *J. Sci. Instrum.* **34** (1957), 399.
- [2] YODER P. R., HOLLIS W. W., *J. Opt. Soc. Am.* **47** (1957), 858.
- [3] DUCHOPEL I. I., *Opt. Mech. Prom.*, No. 9, (1971), 63 (in Russian).
- [4] SCHULTZ G., SCHWIDER J., *Interferometric testing of smooth surfaces*, [In] *Progress in Optics*, [Ed.] E. Wolf, Amsterdam 1976, Vol. 13, pp. 93–167.
- [5] MALACARA D. [Ed.], *Optical Shop Testing*, Wiley, New York 1978, Chapt. 1.
- [6] RODIONOV S. A., AGUROK I. P., *Opt. Mech. Prom.*, No. 8 (1988), 3 (in Russian).
- [7] KOGELNIK H., LI T., *Appl. Opt.* **5** (1966), 1550.
- [8] JÓZWICKI R., *Optic* **62** (1982), 231.
- [9] JÓZWICKI R., *Theory of Optical Imaging* (in Polish), PWN, Warszawa 1988, Sect. 2.3.4.
- [10] BORN M., WOLF E., *Principles of Optics*, Pergamon Press, Oxford 1980.
- [11] BRACEWELL R., *The Fourier Transform and Its Applications*, McGraw–Hill, New York 1965, Table 12.1.
- [12] PAPOULIS A., *Systems and Transforms with Applications in Optics*, McGraw–Hill, New York 1968, Chapt. 9.
- [13] STOLER D., *J. Opt. Soc. Am.* **71** (1981), 334.
- [14] HOPKINS H. H., *Wave Theory of Aberrations*, Clarendon, Oxford 1950, Chapt. 4.
- [15] JÓZWICKI R., *Opt. Acta* **29** (1982), 1383.
- [16] JÓZWICKI R., *Opt. Acta* **30** (1983), 73.
- [17] MCLACHLAN N. W., *Bessel Functions for Engineers*, Clarendon, Oxford 1955 (see list of the formulae).

*Received March 22, 1990
in revised form May 5, 1990*

Распространение абберационной волны с неоднородным распределением амплитуды и его влияние на точность интерференционных измерений

В интерферометрах с разностью оптических путей неравной нулю две распространяющиеся волны изменяются по-разному. Разность форм волновых фронтов определяет ошибку, связанную с абберацией. В статье получены формулы в дифференциальной форме, описывающие распространение волны с плоскими или сферическими фронтами. Полученные результаты сравнены с формулой для пучка Эри. Предложена разветка оптической системы интерферометра по отношению к зеркальным элементам. Проанализировано влияние неоднородного освещения и абберации третьего порядка. Рассмотрен случай гауссовской абсорбции. Получена формула, описывающая ошибки, внесенные посредством абберации распространяющейся волны. Выведены корректные критерии для сферической абберации. Обнаружена связь с угловой абберацией.